Available online at www.sciencedirect.com
SCIENCE DIRECT®
Journal of Chromatography A, 1013 (2003) 35–45
JOURNAL OF CHROMATOGRAPHY A
www.elsevier.com/locate/chroma

Capillary electrochromatography with monolithic stationary phases II. Preparation of cationic stearyl-acrylate monoliths and their electrochromatographic characterization☆

Mohamed Bedair, Ziad El Rassi*
Department of Chemistry, College of Arts and Sciences, 454A Physical Sciences, Oklahoma State University, Stillwater, OK 74078-3071, USA

Abstract

A novel cationic monolithic stationary phase based on the co-polymerization of pentaerythritol diacrylate monostearate (PEDAS) with a selected quaternary amine acrylic monomer was designed for performing capillary electrochromatography at high flow velocity. While PEDAS functioned as both the ligand provider and the cross-linker, the quaternary amine acrylic monomer was introduced to control the magnitude of the electroosmotic flow (EOF). The fabrication of the cationic stearyl-acrylate monolith (designated as cationic C_{17} monolith) with controlled porosity was achieved by free radical polymerization using the initiator 2,2′-azobisisobutyronitrile in the presence of a ternary porogenic solvent composed of cyclohexanol, ethylene glycol and water. Four different quaternary amine acrylic monomers were investigated in order to find the optimum monomer for achieving maximum electroosmotic flow (EOF) velocity. Both photo- and thermally-initiated polymerization proved effective in producing the cationic C_{17} monolith, and the best monolith was achieved when [2-(acryloyloxy)ethyl]trimethyl ammonium methyl sulfate (AETA) was used as the quaternary amine acrylic monomer. Although the zeta potential of the resulting cationic C_{17} monolith is positive with respect to water, the magnitude and direction of the EOF was markedly affected by the nature of the electrolyte in the mobile phase. Consequently, anodal, zero or cathodal EOF was observed depending on the nature of the electrolyte, and this was attributed to the adsorption of the ionic components of the electrolyte on to the solid stationary phase, which is characterized by its amphiphilic nature consisting of C_{17} chains, ester functions, hydroxyl groups and quaternary amine moieties. Optimized PEDAS–AETA monoliths yielded columns with high separation efficiency and allowed rapid separations on the time scale of seconds to be achieved with short capillaries.

Keywords: Monolithic columns; Stationary phases, electrochromatography; Stearyl-acrylate monoliths; Electroosmotic flow; Polymerization; Electrochromatography

1. Introduction

Capillary electrochromatography (CEC) with monolithic capillary columns is becoming a promising separation method by virtue of the ease with which the monoliths can be produced and confined in capillaries and the vast available chemistries that can facilitate the in situ polymerization of tailor-made

☆Presented also as a part of an oral presentation at HPLC 2002, Montreal, Canada, 2–7 June, 2002.

*Corresponding author. Tel.: +1-405-744-5931; fax: +1-405-744-6007.
E-mail address: zelrassi@biochem.okstate.edu (Z. El Rassi).

0021-9673/03/$ – see front matter
doi:10.1016/S0021-9673(03)01031-8

monoliths with controlled porosity and well-defined retentive properties. These features make the monolithic stationary phases the most convenient approach for exploiting the hybrid separation mechanism of CEC for achieving rapid and efficient separations. In fact, CEC combines the separation mechanisms of capillary electrophoresis and micro-HPLC, which are the most advanced and universal micro-column separation techniques available nowadays. Although significant advances have been made in the design of monolithic stationary phases for CEC (for recent review articles see Refs. [1–5]), the exploitation of the full potentials of monolithic columns in CEC requires further development in order to accommodate the separations of a wide range of small and large species. Typical polymeric monoliths include acrylamide-based porous polymers prepared from aqueous solutions [6], highly cross-linked acrylamide-based monoliths [7], acrylamide-based monoliths prepared in the presence of organic solvents [8,9], polystyrene-based polymers [10] and methacrylate ester-based monolithic columns [11,12]. In a recent report, we introduced a novel anionic stearyl-acrylate monolith to address the need for monoliths with long alkyl chains (C_{17}) at high flow velocity, which afford sufficient retention and selectivity towards various neutral and charged species [13]. These anionic C_{17} monoliths are based on the copolymerization of pentaerythritol diacrylate monostearate (PEDAS) with 2-acrylamido-2-methyl-1-propanesulfonic acid (AMPS). As a continuation of our investigation in monoliths specially designed for CEC, we are proposing here a cationic C_{17} monolith based on the copolymerization of PEDAS and an acrylic monomer with a quaternary amine function with the aim of producing stationary phases that allow the separation of positively charged species and show little or no electrostatic interactions with proteins.

This report is concerned with the optimization of the fabrication of the cationic C_{17} monolith in terms of the composition of the polymerization mixture, the nature of the quaternary amine acrylic monomer and the composition of the porogenic solvent. The resulting cationic monoliths were electrochromatographically characterized over a wide range of elution conditions in terms of magnitude and direction of the electroosmotic flow (EOF) and the separation efficiency at various linear flow velocities using two homologous series, namely alkyl benzenes and alkyl phenyl ketones as the test solutes. The evaluation of the electrochromatographic retention of neutral and charged species including water-soluble proteins and membrane proteins are the subject of part III of this series.

2. Experimental

2.1. Instrumentation

The instrument used was a $HP^{3D}CE$ system from Hewlett-Packard (Waldbronn, Germany) equipped with a photodiode array detector. Electrochromatograms were recorded with a personal computer running a $HP^{3D}CE$ Chemstation. A pressure of 1.0 MPa (i.e. 10 bar) was applied to both ends of the capillary during the experimental runs to minimize bubble formation. The temperature was held constant at 25 °C. All samples were injected electrokinetically at various times and applied voltages, which are stated in the figure captions.

2.2. Reagents and materials

Pentaerythritol diacrylate monostearate (PEDAS), [2 - (methacryloyloxy) ethyl] trimethylammonium methylsulfate (META), [2-(acryloyloxy)ethyl]trimethylammonium methylsulfate (AETA), (3-acrylamidopropyl)trimethylammonium chloride (APTA), [2 - (methacryloyloxy) ethyl] trimethylammonium-chloride (MAETA), 2,2′-azobisisobutyronitrile-(AIBN), 3-(trimethoxysilyl)propylmethacrylate, *N*-[3 - (trimethoxysilyl)propyl] - *N*′ - (4 - vinylbenzyl ethylenediamine hydrochloride, alkylbenzenes, alkyl phenyl ketones, ethylenediamine (EDA), triethylenetetraamine (TETA), tetrabutylammonium bromide (TBAB) and analytical grade acetone were purchased from Aldrich (Milwaukee, WI, USA). Cyclohexanol was purchased from J.T. Baker (Phillipsburg, NJ, USA). Sodium phosphate monobasic and dibasic and sodium acetate were from Mallinckrodt (Paris, KY, USA). Ethylene glycol and HPLC-grade methanol and acetonitrile were from Fisher Scientific (Fair Lawn, NJ, USA). 2-(*N*-Morpholino)ethanesulfonic acid (MES), Tris, Bis–Tris and Bis–Tris propane were purchased from Sigma

(St. Louis, MO, USA). Fused-silica capillaries with an internal diameter of 100 μm and an outer diameter of 360 μm were from Polymicro Technology (Phoenix, AZ, USA).

2.3. Column pretreatment

The inner wall of the fused-silica capillary was treated with 1.0 *M* sodium hydroxide for 30 min, flushed with 0.10 *M* hydrochloric acid for 30 min, and then rinsed with water for 30 min. The capillary inner wall was then allowed to react with either a 50% (v/v) solution of 3-(trimethoxysilyl)propyl methacrylate in acetone or a 50% (v/v) solution of *N*-[3-(trimethoxysilyl)propyl]-*N′*-(4-vinylbenzyl)-ethylenediamine hydrochloride in methanol for 12 h to vinylize the inner wall of the capillary. This bifunctional silane was first used by Ngola et al. to functionalize the walls of fused-silica capillaries prior to in situ polymerization of monoliths inside the capillaries [12]. Finally, the capillary was rinsed with methanol and water and dried with a stream of nitrogen.

2.4. In situ polymerization

Polymerization solutions weighing 1.6 g each were prepared from monomers, e.g. PEDAS monomer and a quaternary amine monomer (see Table 1), and porogenic solvents in ratios of monomers–solvents (30:70, w/w). The mixtures of monomers were dissolved in ternary porogenic solvents consisting of 75.4% (w/w) cyclohexanol, 21% (w/w) ethylene glycol (EG) and 3.6% (w/w) water [13]. AIBN or benzoin methyl ether (1.0%, w/w, with respect to monomers) was added to the solution as initiator. The solution was then sonicated to obtain a clear solution, and to free the solution from dissolved air.

A 40-cm length of the pretreated capillary (see Section 2.3) was filled with the polymerization solution up to 30 cm (for a 25 cm effective monolithic column length) or 12 cm (for an 8.5 cm effective monolithic column length) by immersing the inlet of the capillary into the solution vial and applying a negative pressure (i.e. sucking with a syringe) to the outlet. The capillary ends were then sealed in an oxygen flame, and the capillary submerged in a 60 °C water bath for 18 h. Photoinitiated polymerization was carried out using UV-transparent capillaries. The capillaries were irradiated with an 8-W UV lamp (EN180, Spectronics, USA) at 365 nm from a distance of 7.5 cm at room temperature for various amounts of time.

The resulting monolithic column was washed with acetonitrile–water (80:20, v/v) mixture using a HPLC pump. A detection window was created at 1–2 mm after the end of the polymer bed using a thermal wire stripper. Finally, the column was cut to a total length of 33.5 cm with an effective length of 25 cm or 8.5 cm.

Table 1
Composition of the polymerization solutions used in the preparation of the different monolithic columns. Capillary column, 33.5 cm (25 cm effective length)×100 μm I.D.; mobile phase, 1.0 m*M* sodium monophosphate, pH 3.0, at 80% (v/v) acetonitrile; voltage, −25 kV

Column/monolith designation	Quaternary amine monomer		Plates/m	EOF (mm/s)	k' of amyl benzene
	Designation	% (w/w)[a]			
A	APTA	1.4	32 000	0.56	2.09
B	MAETA	3.6	7000	1.21	2.04
C	META	3.2	54 000	1.77	1.73
D	AETA	3.2	123 000	2.44	2.15
E	AETA	2.0	126 000	2.46	1.99
F	AETA	1.6	125 000	2.45	1.99
G	AETA	0.6	138 000	2.42	2.14
H	AETA	0.3	81 000	1.98	2.08
I	AETA	0.25	105 000	1.75	2.19

[a] Percentage of quaternary amine monomer used in the polymerization mixture.

3. Results and discussion

3.1. Column construction

3.1.1. Choice of the porogens

To produce a permanent porosity in a polymeric monolith, the in situ polymerization is usually performed in the presence of porogens, which produce phase separation of the solid polymer from the liquid porogens. In a recent contribution from our laboratory [13], a ternary porogenic solvent consisting of cyclohexanol, ethylene glycol and water has been shown very effective in pore tailoring of sulfonated acrylic monoliths. This ternary porogen (75.4%, w/w, cyclohexanol, 21%, w/w, ethylene glycol (EG) and 3.6%, w/w, water) was also used in the present investigation. Preparing a column in the presence of a porogen consisting of only cyclohexanol and ethylene glycol assessed the need for including water in the polymerization reaction. The column thus obtained gave relatively low separation efficiency. Using a higher amount of water than 3.6% (w/w) (e.g. 6.85%, w/w, of porogen composition) in the porogen caused a solubility problem to the PEDAS monomer. Similarly, a higher amount of ethylene glycol than 21% (w/w) of porogen caused a solubility problem for the PEDAS monomer, while a lower amount produced columns which were not permeable enough to flush using a HPLC pump.

3.1.2. Composition of the polymerization mixture

Polymerization solutions with monomer-to-solvent ratio of 30:70 (w/w) were used since they proved to be the optimal composition in previous studies [13] with anionic stearyl-acrylate monoliths. In fact, increasing the monomer-to-solvent ratio to 36.6:63.4 increased the polymer crosslinking, which lowered the efficiency of the column dramatically from 125 000 plates/m (exhibited by column F, see Table 1) to 24 000 plates/m.

PEDAS was used as the crosslinker and the C_{17} ligand provider at the same time, while an acrylate with a quaternary amine group was used as the charged monomer to provide an anodic EOF. In this regard, four different quaternary amine monomers were tested (see Table 1 and Fig. 1) in order to select the monomer that would yield the highest EOF velocity and monolith permeability. As shown in Table 1, AETA gave the highest plate count and EOF velocity, and was used in further studies. This is indicative of the difference in reactivity among the various quaternary amine monomers tested.

Increasing the amount of AETA from 0.25 to 0.60% (w/w) of monomer composition in the polymerization mixture led to a sharp increase in the

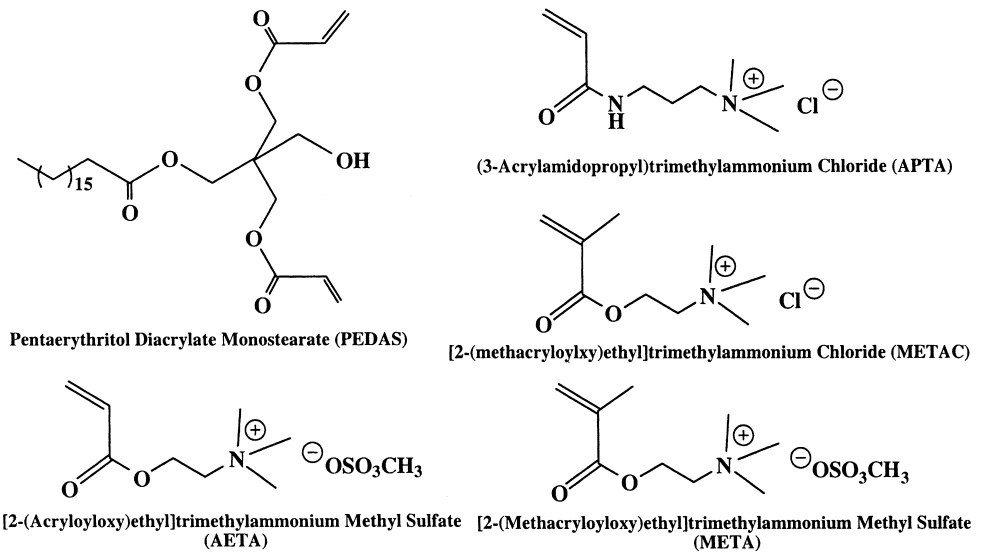

Fig. 1. Structures, chemical names and abbreviations of monomers used in this study.

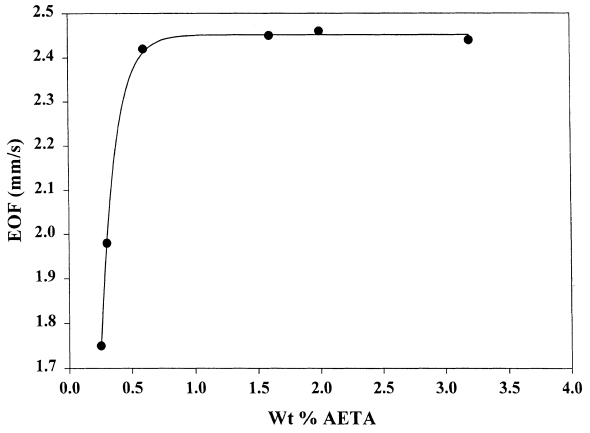

Fig. 2. Effect of % (w/w) of AETA in the polymerization solution on the apparent EOF velocity. Capillary column, 33.5 cm (25 cm effective length)×100 μm I.D.; mobile phase, 1 m*M* sodium phosphate, pH 3.0, at 80% (v/v) acetonitrile; running voltage, −25 kV.

EOF of the monoliths from 1.75 to 2.42 mm/s (Fig. 2). As can be seen in Fig. 2, increasing the % (w/w) of AETA beyond 0.60% (w/w) did not significantly yield further increase in the EOF velocity of the monolith, indicating a saturation level of the amount of AETA that can be incorporated into the PEDAS monoliths.

3.1.3. Bifunctional silane

To anchor a monolithic stationary phase to the capillary inner wall, a bifunctional organosilane is usually used to coat the capillary inner wall prior to the in situ polymerization of the desired monolith inside the capillary. The contribution of the positively charged bifunctional silane, *N*-[3-(trimethoxysilyl)propyl] - *N′* - (4 - vinylbenzyl)ethylenediamine hydrochloride, to the overall EOF exhibited by the monoliths was assessed as follows. One capillary was pretreated with the neutral bifunctional silane, 3-(trimethoxysilyl)propyl methacrylate, while the inner wall of a second capillary was coated with the positively charged bifunctional silane *N*-[3-(trimethoxysilyl)propyl] - *N′* - (4 - vinylbenzyl)ethylenediamine hydrochloride. Both capillaries were filled with the same monolith by in situ polymerization of the monomers used to produce column G, see Table 1. The two monolithic columns were evaluated under the same running conditions (see Table 2) with

Table 2
Effect of the nature of the bifunctional silane used in coating the capillary walls (i.e. monolith-capillary wall binder) on EOF and the column separation efficiency measured with alkyl benzene homologous series. The composition of the monolith was that of column G. Capillary column, 33.5 cm (25 cm effective length)× 100 μm I.D. The mobile phase was 1.0 m*M* sodium phosphate, pH 3.0 or 1.0 m*M* Bis–Tris, pH 6.0 or 1.0 m*M* Bis–Tris propane, pH 7.0, at 80% (v/v) acetonitrile; voltage, −25 kV

pH of the mobile phase	Quaternary amine coated capillary		Neutral coated capillary	
	EOF (mm/s)	*N* (plates/m)	EOF (mm/s)	*N* (plates/m)
3.0	2.46	120 000	2.31	105 000
6.0	1.01	133 000	0.93	115 000
7.0	1.21	149 000	1.05	133 000

mobile phases having three different pH values and consisting of 1 m*M* sodium phosphate monobasic (pH 3.0), 1 m*M* Bis–Tris (pH 6.0) and 1 m*M* Bis–Tris propane (pH 7.0). Under these conditions, the EOF velocity decreased by ~6%, ~8% and ~13% when replacing the positively charged bifunctional silane with the neutral bifunctional silane at pH 3, 6 and 7, respectively (see Table 2). Although the contribution of the positively charged bifunctional silane to the apparent EOF is small, its presence yielded monolithic columns with higher plate counts by ~12 to ~16% when compared to monolithic columns having neutral bifunctional silane on their inner walls (see Table 2). This may indicate that the EOF profile is more uniform (in the radial direction) when the capillary wall is coated with the positively charged bifunctional silane than with its neutral counterpart.

3.1.4. Photo- versus thermally-initiated polymerization

In photo-initiated polymerization, AIBN was also used as the free radical initiator. The effect of reaction time on the retentive property and EOF velocity of the column prepared by AIBN photo-initiated polymerization was studied. The photo-initiated columns have the same composition as that of the thermally-initiated column G (see Table 1) in terms of monomers, porogen and initiator except columns J, K and L, which have different porogen composition (see Table 3). As shown in Fig. 3, the EOF increases sharply when going from 1.5 to

Table 3
Composition, reaction conditions and separation efficiencies for monolithic columns prepared by photo-initiated polymerization. Capillary column, 33.5 cm (25 cm effective length)×100 μm I.D.; separation efficiency was measured with alkyl benzene homologous series; mobile phase, 1.0 m*M* sodium monophosphate, pH 3.0, at 80% (v/v) acetonitrile; voltage, −25 kV

Column	Composition of porogenic solvent			Reaction time (h)	Plates/m
	Cyclohexanol	Ethylene glycol	Water		
G1				1.5	75 000
G2				3.0	94 000
G3	75.20	21	3.8	6.0	76 000
G4				9.0	106 000
G5				12.0	17 000
G6				18.0	Column could not be rinsed
J	85.97	10.11	3.92	9.0	121 000
K	91.01	4.94	4.04	9.0	91 000
L	96.10	0	3.9	9.0	Transparent polymer

3 h of reaction time (i.e. UV irradiation time) and then somewhat levels off, thus indicating an increase in the amount of co-polymerized AETA in the monolith. Conversely, the retention factor k' of amyl benzene decreases sharply when going from 1.5 to 3 h of UV irradiation time and then levels off, thus reflecting an increase in the charged monomer in the polymer matrix as the irradiation time is increased from 1.5 to 3 h. The EOF velocity of photo-initiated columns obtained after 6 to 9 h of UV irradiation is about the same as that of thermally-initiated columns, but the separation efficiency for the former is lower than for the latter. This agrees well with recent findings [14] that monoliths prepared by thermal polymerization exhibited better electrochromatographic properties than monoliths prepared by photo polymerization. Nine hours of UV irradiation time seem to produce a good monolith with the highest separation efficiency as tested with the alkyl benzene homologous series.

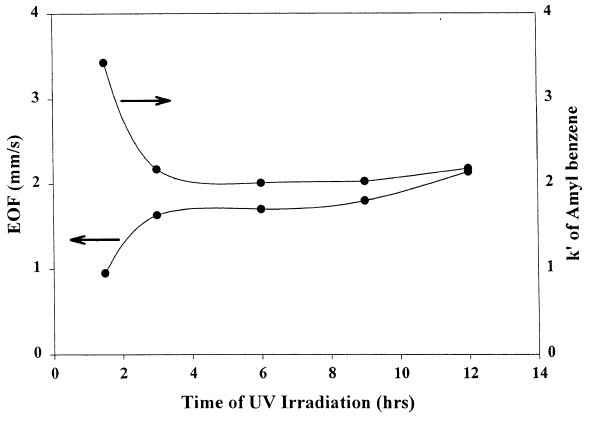

Fig. 3. Plots of the apparent EOF velocity and the retention factor of amyl benzene as a function of the reaction time of photo-polymerization. Monolithic columns G1 to G5 were used. Capillary column, 33.5 cm (25 cm effective length)×100 μm I.D.; mobile phase, 1 m*M* sodium phosphate, pH 3.0, at 80% (v/v) acetonitrile; running voltage, −25 kV.

The permeability of the photo-initiated columns was less than in the case of thermally-initiated columns as was indicated by the pressure drop generated when rinsing the column with a HPLC pump. Also, the permeability decreased with the time of the reaction. In fact, for the 18 h photo-initiated reaction, the resulting column (column G6) could not be rinsed with a HPLC pump and no hydraulic flow could be achieved. In addition, the separation efficiency of the column decreased with increasing reaction time (17 000/m for 12 h reaction, see Table 3) probably due to a higher cross-linking and increased microporosity. The smaller pore size generated by photo-initiated polymerization compared to thermally-initiated polymerization was also assessed from the steeper slope of the Van Deemter plot obtained with column G4 at high EOF velocity (results not shown) as compared to column G. It has been recently shown that the porogen used for thermal polymerization may not be the best suited for photo-initiated polymerization due to the different solubility of the polymer aggregate at different temperature [15], since the photo-initiated polymerization is conducted at room temperature. On this

basis, the porogen composition was then changed to improve the solubility of the polymer aggregate. The % (w/w) of cyclohexanol in the porogen composition was increased and the % (w/w) of ethylene glycol was decreased, while the % (w/w) of water was kept constant, see Table 3. Columns J and K with ~10 and ~5% (w/w) of ethylene glycol, respectively, showed higher permeability in HPLC rinsing and higher EOF flow compared to column G4. The presence of ethylene glycol was found essential in the porogenic solvent since its absence produced a nonporous transparent polymer (column L). It seems that the porogen composition for column J yields higher separation efficiency than any other photo-initiated monolith (see Table 3). Also, column J has very close performance to column G produced by thermal polymerization. Therefore, cationic stearyl-acrylate monoliths can be produced more or less equally well by photo- or thermally-initiated polymerization when using the proper porogen composition. Although thermally-initiated monoliths exhibited slightly better performance in terms of separation efficiency, the photo-initiated monolith can be produced at a higher rate (shorter time; 9 h as opposed to 18 h by thermal polymerization) and can be performed in any specified space, e.g. chip-based microfluidics, since the UV irradiation can be restricted to the desired areas by using masks that shield the other areas from UV irradiation [16,17].

3.1.5. Reproducibility of column fabrication

The reproducibility of column fabrication was assessed through the percent relative standard deviation (RSD) for the EOF velocity, solute retention and separation efficiency using alkyl benzene homologous series as the model solutes. Typically, the observed RSDs from column-to-column ($n=3$) for column G were 1.22%, 4.4% and 8.1% for the retention factor, EOF velocity and separation efficiency, respectively. These reproducibility data are comparable to what we reported before for a similar monolith [13], and are in close agreement with those recently reported in the literature [18].

3.2. Column characterization and performance

3.2.1. Magnitude and direction of EOF

The dependence of the magnitude and direction of the apparent EOF on the pH of the mobile phase was examined in the pH range 2.5–7.0 using the monolithic column G and various electrolytes at 80% (v/v) acetonitrile (Fig. 4). The monoliths under investigation possess a positive zeta potential with respect to water due to the presence of the quaternary amine monomer AETA, which is co-polymerized with PEDAS. Under these circumstances, the monolithic capillary column should yield an anodal EOF provided that its positive zeta potential is not markedly altered by the mobile phase ions. As can be seen in Fig. 4, the direction and magnitude of the EOF depends largely on the nature of the electrolyte used in the mobile phase. This is indicative of the adsorption of electrolyte ionic components onto the solid stationary phase surface, thus becoming the zeta potential determining ions (i.e. determining the sign of the surface zeta potential), and consequently the direction of the EOF. The effect of the adsorption of ions on the zeta potential of solid phases is a long-known well-documented phenomenon for non-ionized solids (e.g. certain plastics) and ionizable solids (e.g. silica, ion-exchange resins, agar, etc.; see Ref. [19]). The surface of the acrylic monolith under investigation is an ester-rich surface having hydroxyl groups, quaternary amine functions and non-polar C_{17} moieties (see Fig. 1). This amphiphilic surface has the potential to adsorb ions from solution via various interactions including hydrogen bonding, electrostatic attractions and van der Waals interactions. Also, one cannot exclude some trapping of ions in the polymeric network. As can be seen in Fig. 4, a quasi-constant anodal EOF can be achieved in the pH range 2.5 to 7.0 by using electrolytes containing sodium phosphate at pH 2.5 and 3.0 and polyamines/quaternary amine as the co-ions e.g. ethylene diamine (EDA) or triethylenetetraamine (TETA)–tetrabutylammonium bromide (TBAB), in the pH range 4.0 to 7.0. At pH 2.5 and 3.0, sodium phosphate seems to maintain or not significantly alter the ‘‘proper’’ positive zeta potential of the monolithic surface, which originates from the AETA monomer. However, at pH 4.0, 6.0 and 7.0, sodium phosphate seems to produce a negative zeta potential as manifested by the cathodal EOF of different magnitude. While the electrolyte EDA–HCl, pH 4.0, produces a relatively strong anodal EOF, substituting the EDA–HCl by EDA–acetic acid reduces the

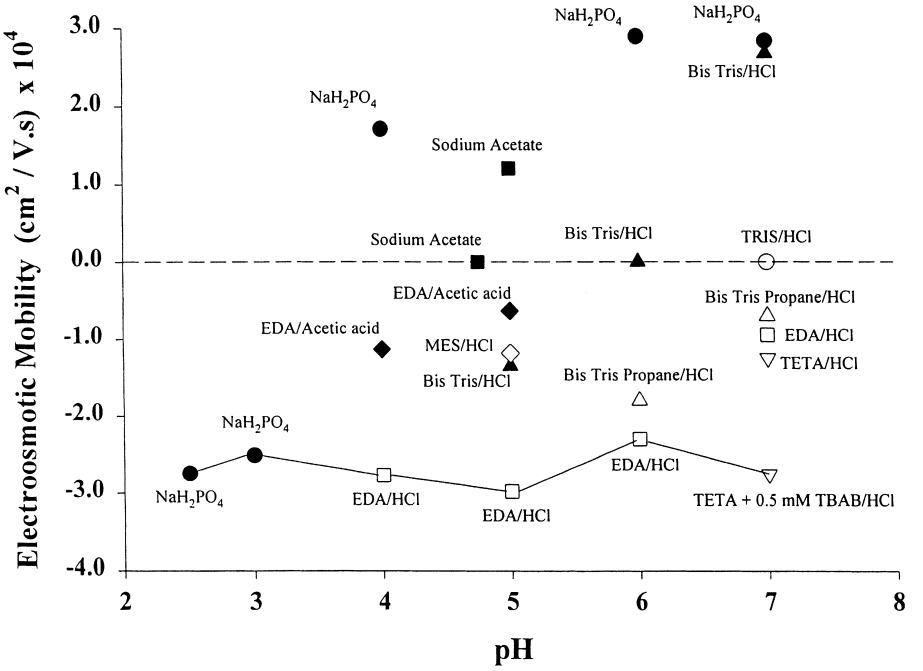

Fig. 4. Plots of the apparent EOF velocity versus the pH of the mobile phase. Capillary column G, 33.5 cm (25 cm effective length)×100 μm I.D.; mobile phases, 1 m*M* buffer at 80% (v/v) acetonitrile; running voltage, ±25 kV.

anodal EOF by half (see Fig. 4). This seems to indicate that the acetate counter-ion adsorbs to the surface thus reducing the magnitude of the positive zeta potential. The EDA–HCl produced more or less the same EOF at pH 4.0 and 5.0, which gradually decreased as the pH was changed to 6.0 and 7.0 (see Fig. 4). Substituting EDA–HCl by TETA–HCl yielded a slightly higher anodal EOF at pH 7.0. The addition of a small amount of tetrabutyl ammonium bromide helped—boosting the EOF to approach what is obtained with phosphate at pH 2.5 and 3.0 (see Fig. 4). Bis–Tris, which yielded an anodal EOF at pH 5.0, failed to produce any flow at pH 6.0 and the flow reverted to cathodal at pH 7.0. Tris–HCl did not produce any flow at pH 7.0. Sodium acetate did not allow any measurable EOF at pH 4.75 and reverted the direction of the EOF at pH 5.0.

The cationic stearyl acrylate monolith exhibits anodal, ‘‘zero’’ and cathodal EOF depending on the nature of the mobile phase electrolyte. The tri-directional EOF represents an advantage as far as the manipulation of elution orders, resolution, efficiency and speed of separation are concerned.

3.2.2. Van Deemter plots

In a recent study [13], we have shown that a Van Deemter plot is a useful tool for probing in the porosity of monolithic stationary phases. Fig. 5 compares the Van Deemter plots obtained on three monolithic columns, which were obtained from polymerization reactions at 0.3% (w/w) (column H, Fig. 5a), 0.6% (w/w) (column G, Fig. 5b) and 2.0% (w/w) AETA (column E, Fig. 5c). Also, to probe into the relative presence of micropores in each of these monoliths, the Van Deemter plots were constructed at various mobile phase ionic strengths. In all cases, the plate height was measured as a function of apparent EOF velocity by varying the applied voltage. The hyperbolic shape of the curves resembles those reported in the literature with other types of polymer-based monoliths [12,13,18]. Increasing the amount of the charged monomer in the polymerization mixture not only increases the surface charge density of the monolith and in turn the EOF velocity (see Fig. 2) but also results in an increase in the mode pore diameter [18]. As can be seen in Fig. 5a, column H which was prepared from a poly-

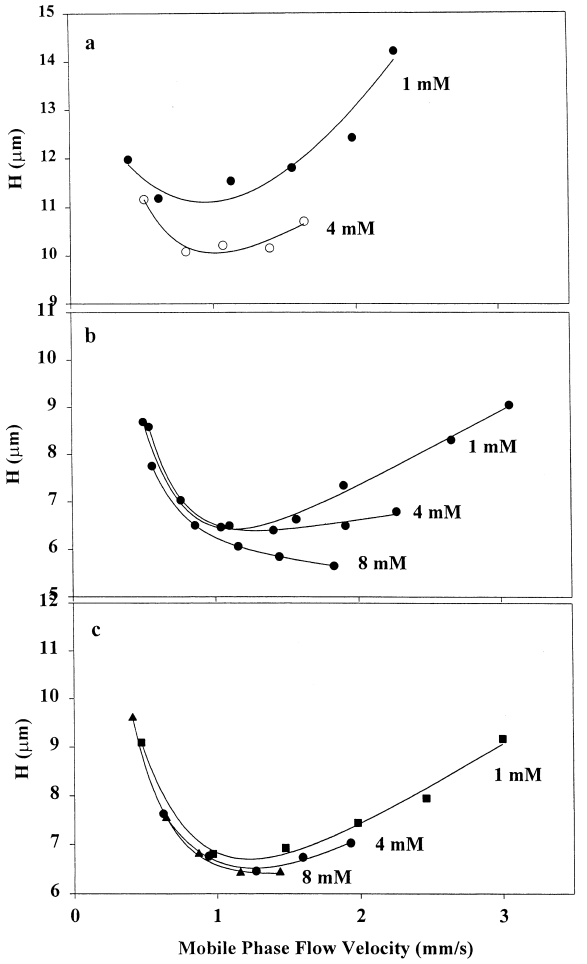

Fig. 5. Van Deemter plots showing average plate height as a function of apparent mobile phase flow velocity for various monolithic columns prepared from polymerization solution at different % (w/w) AETA. (a) Column H, (b) column G, (c) column E. The plate height is the average taken for the first six alkylbenzene homologous series. Capillary column, 33.5 cm (25 cm effective length)×100 μm I.D.; mobile phase, 1.0, 4.0 or 8.0 m*M* sodium phosphate, pH 3.0, at 80% (v/v) acetonitrile; electrokinetic injection, −10 kV for 2 s.

merization mixture at 0.3% (w/w) AETA yielded the lowest separation efficiency and especially at high flow velocity, a behavior that is typical of microporous stationary phase. Micropores bring about high mass transfer resistance at high flow velocity and in turn low separation efficiency. The separation efficiency was improved upon increasing the mobile phase ionic strength which may indicate that column H contains a large amount of micropores whereby at low ionic strength an extensive double layer overlap takes place, thus inhibiting flow through pore (i.e. perfusive flow) and in turn higher mass transfer resistance would result, which becomes significant at high flow velocity. Incorporating into the polymerization mixture 0.6% (w/w) AETA (column G) improved the separation efficiency, which may indicate a decrease in the microporosity of the monolith. Column G may still have some microporosity as manifested by the increase in separation efficiency at high ionic strength. Although increasing the % (w/w) of AETA beyond 0.6% (w/w) did not increase the magnitude of EOF (see Fig. 2), using a polymerization at 2.0% (w/w) AETA yielded a column E with much less micropores than column H and column G as manifested by the little effect of ionic strength on the separation efficiency.

3.2.3. Column performance

Two homologous series, namely alkyl benzenes (highly hydrophobic) and alkyl phenyl ketones (APKs, moderately hydrophobic) were used to evaluate the monolithic columns. Figs. 6 and 7 show typical electrochromatograms obtained on a long column (25 cm effective length) and a short column (8.5 cm effective length), respectively. As shown in Fig. 6, and as expected, APK exhibited less retention than the alkyl benzene under otherwise the same conditions. An important feature is that a short column of 8.5 cm not only permitted the ultra-fast separation of six alkyl benzene solutes in less than 60 s (see Fig. 7) but also exhibited high separation efficiency. In fact, shortening the column length by a factor of ~2.9 and increasing the flow velocity by a factor of ~1.6 did decrease the average plate number per meter by only a factor of ~1.4. However, the short column (8.5 cm) produced ~159 plates/s as opposed to ~100 plates/s for the longer column (25 cm).

4. Conclusions

We have shown that cationic stearyl-acrylate monolithic stationary phase can be readily confined in capillary columns either via photo- or thermally-initiated polymerization. A ternary porogenic solvent

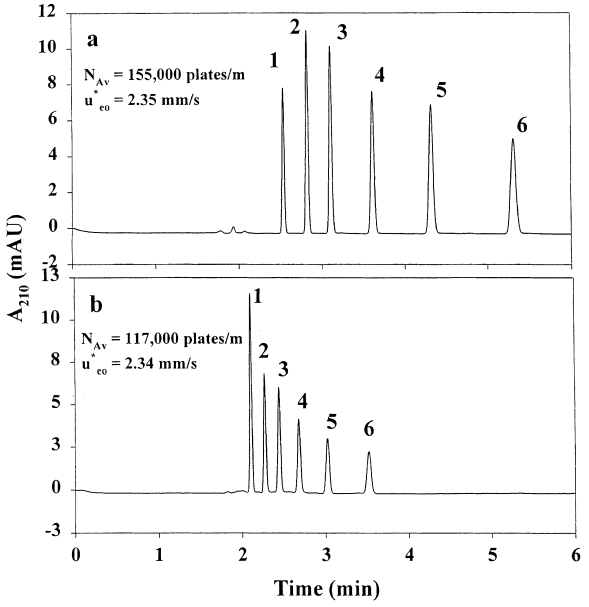

Fig. 6. Electrochromatograms of (a) alkylbenzene and (b) alkyl phenyl ketones homologous series obtained on monolithic column G, 33.5 cm (25 cm effective length)×100 μm I.D.; mobile phase, 1 m*M* sodium phosphate, pH 3.0, at 80% (v/v) acetonitrile; running voltage, −25 kV; electrokinetic injection, −10 kV for 2 s. Solutes (a): 1, benzene; 2, toluene; 3, ethylbenzene; 4, propylbenzene; 5, butylbenzene; 6, amylbenzene. Solutes (b): 1, acetophenone; 2, propiophenone; 3, butyrophenone; 4, valerophenone; 5, hexanophenone; 6, heptanophenone.

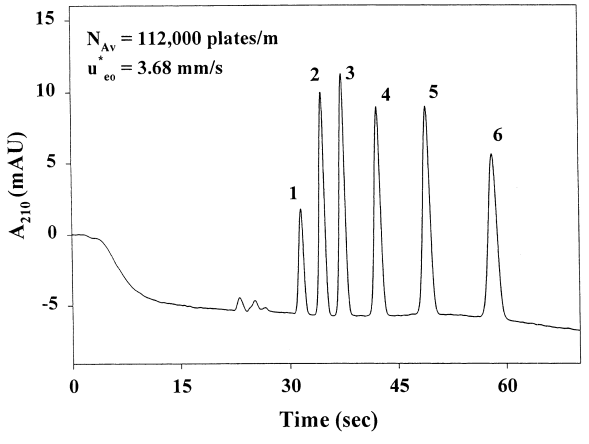

Fig. 7. Ultra fast separation of alkyl benzene homologous series obtained on monolithic column G, 33.5 (8.5 cm effective length)× 100 μm I.D.; mobile phase, 1 m*M* sodium phosphate, pH 3.0 at 82% (v/v) acetonitrile; running voltage, −30 kV; electrokinetic injection, −10 kV for 2 s. Solutes: 1, benzene; 2, toluene; 3, ethylbenzene; 4, propylbenzene; 5, butylbenzene; 6, amylbenzene.

composed of cyclohexanol, ethylene glycol and water proved very efficient in the pore tailoring of the cationic C_{17} monolith. Also important in the pore tailoring process of the cationic C_{17} monolith was the content of the quaternary amine monomer in the polymerization mixture as was revealed from the Van Deemter plots. The sign of the zeta potential of the cationic C_{17} monolith can be manipulated by the nature of the electrolytes to yield anodal, zero or cathodal EOF. By optimizing all the variables pertaining to the fabrication of the cationic C_{17} monolith and the elution conditions, high separation efficiencies were readily obtained and rapid separations on the time scale of seconds were achieved.

Acknowledgements

The financial support from the Environmental Institute/Center for Water Research at Oklahoma State University is gratefully acknowledged.

References

[1] F. Svec, in: Z. Deyl, F. Svec (Eds.), Capillary Electrochromatography, Elsevier, Amsterdam, 2001, p. 183.
[2] E.F. Hilder, F. Svec, J.M.J. Frechet, Electrophoresis 23 (2002) 3934.
[3] C. Legido-Quigley, N.D. Martin, V. Melin, A. Manz, S.W. Smith, Electrophoresis 24 (2003) 917.
[4] N. Tanaka, H. Kobayashi, K. Nakanishi, H. Minakuchi, N. Ishizuka, Anal. Chem. 73 (2001) 420A.
[5] N. Tanaka, H. Kobayashi, in: Z. Deyl, F. Svec (Eds.), Capillary Electrochromatography, Elsevier, Amsterdam, 2001, p. 165.
[6] C. Fujimoto, Anal. Chem. 67 (1995) 2050.
[7] J.-L. Liao, N. Chen, C. Ericson, S. Hjertén, Anal. Chem. 68 (1996) 3468.
[8] A. Palm, M.V. Novotny, Anal. Chem. 69 (1997) 4499.
[9] M. Zhang, Z. El Rassi, Electrophoresis 22 (2001) 2593.
[10] I. Gusev, X. Huang, C. Horvath, J. Chromatogr. A 855 (1999) 273.
[11] E.C. Peters, M. Petro, F. Svec, J.M.J. Frechet, Anal. Chem. 69 (1997) 3646.
[12] S.M. Ngola, Y. Fintschenko, W.-Y. Choi, T.J. Shepodd, Anal. Chem. 73 (2001) 849.
[13] M. Bedair, Z. El Rassi, Electrophoresis 23 (2002) 2938.
[14] M. Lammerhofer, E.C. Peters, C. Yu, F. Svec, J.M.J. Frechet, W. Lindner, Anal. Chem. 72 (2000) 4614.
[15] C. Yu, F. Svec, J.M.J. Frechet, Electrophoresis 21 (2000) 120.

[16] D.S. Peterson, T. Rohr, F. Svec, J.M.J. Frechet, Anal. Chem. 74 (2002) 4081.
[17] C. Yu, M.H. Davey, F. Svec, J.M.J. Frechet, Anal. Chem. 73 (2001) 5088.
[18] E.C. Peters, M. Petro, F. Svec, J.M.J. Frechet, Anal. Chem. 70 (1998) 2288.
[19] C.J.O.R. Morris, P. Morris, in: 2nd ed, Separation Methods in Biochemistry, John Wiley, New York, 1976, p. 718.